Proc. Vth International Workshop, Advances in Signal Processing for Non Destructive Evaluation of Materials
Québec City (Canada),2-4 Aug. 2005. © X. Maldague ed., É. du CAO (2006), ISBN 2-9809199-0-X

Keynote lecture

New approaches to non-destructive evaluation of materials using air-coupled ultrasound

I. Solodov and G. Busse

Institute for Polymer Testing and Polymer Science (IKP) – Department of Non-Destructive Testing, Stuttgart University, Pfaffenwaldring 32, D-70569 Stuttgart, Germany

Abstract

The results of NDE and material characterization with mode conversion of air-coupled ultrasound into plate and surface waves in solids are reported. Single- and both-sided configurations of efficient slanted wave conversion are developed and tested for various materials. An alternative option is based on the excitation of cylindrical plate and surface waves by a focused air-coupled beam incident on a specimen surface. New opportunities of the mode conversion approach are demonstrated in remote mapping of elastic anisotropy, profilometry of thickness, ultrasonic imaging, linear and nonlinear NDE of defects and damage.

Key words: Air-coupled ultrasound, mode conversion, plate waves, surface waves.

1. Introduction

In recent years, air-coupled ultrasound (ACU) has become a routine inspection technique in non-destructive evaluation (NDE) of a wide range of materials and components [1]. However, in conventional ACU-systems, the transmission of ultrasonic energy into solids is extremely inefficient (~10^{-4}) due to the mismatch of acoustic impedances (4-5 orders of magnitude for the majority of materials). The situation is aggravated if, in addition, the materials are laminated, porous or highly dissipative. As a result, NDE with ACU is virtually not possible for “inconvenient” materials, like plastics, foams, some composites, wood, and cement based materials.

To increase the elastic coupling between air and solids, one can use the idea of spatial resonance. The first option includes thickness resonance which strongly enhances vibration amplitude (and ACU transmission) in plate-like samples. Focused ACU beams will produce a resonance area confined around a focus spot which can excite efficiently plate waves in a wide angular range. In slanted ACU configurations, the spatial resonance corresponds to constructive interference of the waves along a particular in-plane direction. In thin samples, this causes a resonance generation of plate acoustic waves (PAW) [2] while an efficient excitation of surface acoustic waves (SAW) is expected when the thickness of the specimen is greater than a few wavelengths.

In this paper, the results of NDE applications based on conversion of focused ACU into plate and surface waves are reported. Unlike conventional scanning ACU systems which are used only for defect imaging, the new applications also include remote profilometry of thickness, mapping of in-plane elastic anisotropy, linear and nonlinear NDE of defects and damage with air-coupled plate and surface waves.

2. Material characterization with ACU conversion

2.1. NDE in focused slanted modes of ACU

In a conventional configuration, the ACU produces a localized surface excitation (membrane-type source) which radiates longitudinal waves inside a solid sample. A synchronous vibration of the source at normal incidence of ACU impedes the wave excitation along the surface. The slanted set-

up enables to introduce an adjustable phase variation and to "stretch" the excitation along the surface. Under phase matching conditions, such a distributed source can operate far more efficiently for the in-plane propagating waves, e.g. PAW, SAW or other types of interface waves. For plane waves, the phase matching depends on the ratio between the velocities of sound in air (v_{air}) and the waves generated ($v_{PAW,SAW}$) which determines the resonance angle of incidence: $(\theta_o)_{PAW,SAW} = \arcsin(v_{air} / v_{PAW,SAW})$. However, real transducers radiate ACU with a finite angular spectrum, so that only a part of the incident energy couples to the waves in a solid. To maximise the air/solid coupling in the slanted configurations, the weakly-focusing ACU transducers are proposed which combine an efficient elastic coupling with a high spatial resolution [3].

The efficiency of conversion also depends on the polarization of the waves excited: ACU coupling is provided only to the out-of-plane components of displacement. According to calculations [4], the out-of-plane displacement dominates in the zero-order anti-symmetric modes in thin plates. For this reason, the conversion efficiency into such flexural waves is usually much higher than that for any other plate wave mode. The surface waves are also polarized mainly out-of-plane so that one would expect their strong coupling to ACU.

The experiments used commercial air-coupled equipment including weakly-focused (focus spot 3-4 mm) 400kHz-piezo-ceramic transducers and a standard scanning table (ISEL-PRO-DIN). The experimental arrangements include Focused Slanted Transmission (FST-) and Focused Slanted Reflection (FSR-) configurations shown in *Figure 1, a.* The former comprises a pair of co-axial ACU weakly focused transducers. The flexural waves excited re-radiate acoustic energy from the reverse side to the receiving transducer thus providing maximum ACU transmission through the specimen at $\theta = \theta_0$. The FSR-set-up uses a similar radiation from the front side of the sample and enables a single-sided access for non-contact inspection.

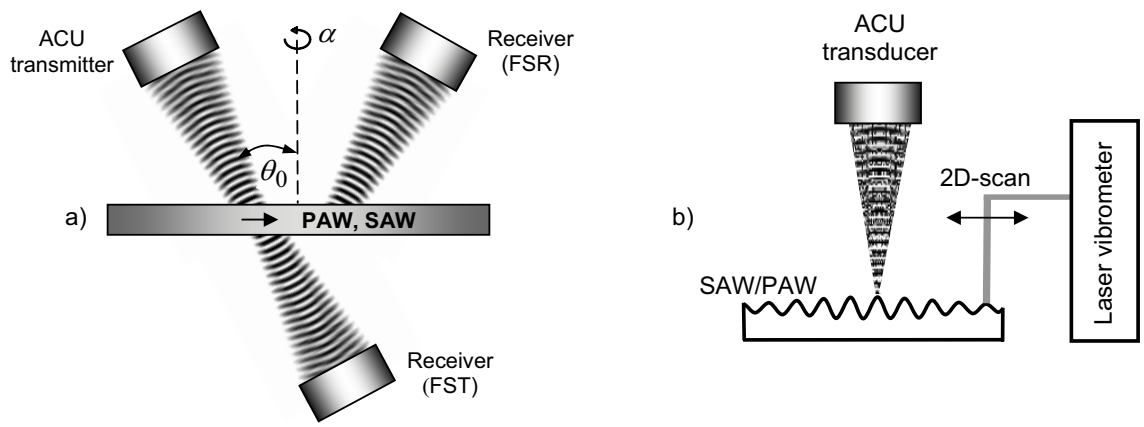

Figure 1. a) - FST- and FSR-configurations; b) – set-up for SAW/PAW wavefront imaging.

2.1.1. Acoustic imaging of defects and profilometry in FS-modes

One of the advantages of using the PAW and SAW for defect imaging is concerned with their strong damping due to scattering by material (and particularly subsurface) inhomogeneities. Besides the increase of acoustic scattering in the defect areas, an additional enhancement of contrast comes from the ACU conversion mechanism: a local variation of θ_0 causes a local drop in the generated (and received) wave amplitudes. The superior amplitude contrast for imaging delaminations in the FS-modes is illustrated in *Figure 2*. It shows ultrasonic scans in normal and slanted transmission of a CFRP laminate (60% fibre content, thickness 4.3 mm) with 4J-low-velocity impact, which induced a 40μm-dent on the front surface as the only visible damage. The damaged

area is well seen in both air-coupled ultrasound scans. However, the FST-image with air-coupled PAW shows a larger area of the induced damage and it also discerns more clearly irregularities in the weave of the carbon fibres in the intact area.

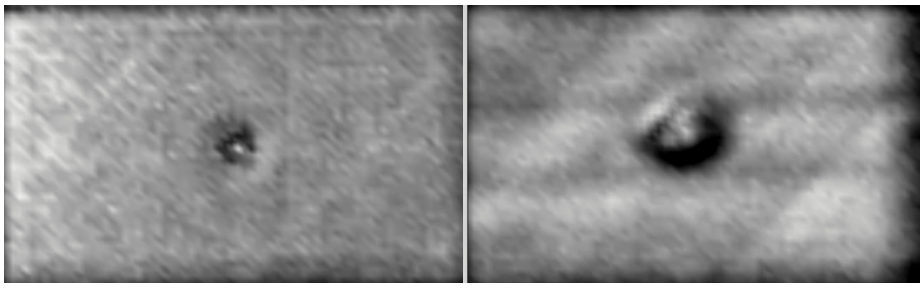

Figure 2. Conventional transmission (left) and FST- (right) scans of impact in CFR-plate (20x15x0.5 cm).

The velocity dependent angular behaviour of the FS-output makes possible a selective conversion of ACU into PAW or SAW which could be applied for NDE of hidden cavities. *Figure 3, c* shows the 2-cm thick Al-sample (30x20 cm) with three cavities of different depths at the bottom side. The thickness of residual material in the cavity areas varies from 1 to 3 mm (*Figure 3).* The results of single-sided scanning (from the intact side) at the resonance angle for ACU excitation of PAW in the 1-mm thick area (*Figure 3, b)* reveal the cavities and enable to distinguish the difference in their depths. The SAW scan exhibits a mirror-inverse contrast with higher output amplitude in parts of regular thickness while the cavities are displayed as low-contrast areas (*Figure 3, a)*.

Since the flexural waves exhibit a strong geometrical dispersion, their velocity depends on the thickness of the specimen. As a result, both the amplitude and the phase of the FST- and FSR-output signals are sensitive to the thickness variation. This property can be used for a remote thickness profilometry of films and coatings using the FS-modes. An example of the FST-B-scanning of inhomogeneous thickness of paint is given in Figure 4. One can see that variation of the delay (phase) of the output signal basically follows the coating profile. The high phase sensitivity of the FST-output to deviation in paint thickness ($\approx 4^0$ / m, Figure 4) confirms a feasibility of high-accuracy profilometry of paint coating on steel substrates typical for automotive industry.

2.1.2. Mapping of in-plane elastic anisotropy in FS-modes

The plane of incidence of ACU in the FS-geometry specifies the direction of wave propagation which can be easily changed by rotating the ACU transducers or the sample (*Figure 1, a*). From measurements of the wave velocity along various directions, the in-plane stiffness anisotropy of a material can be derived. The FS-methodology allows for remote measurements of the in-plane velocity variation by monitoring the changes in the angle of maximum excitation θ_0 or/and phase (φ) of the output air-coupled signal as functions of the azimuth angle α.

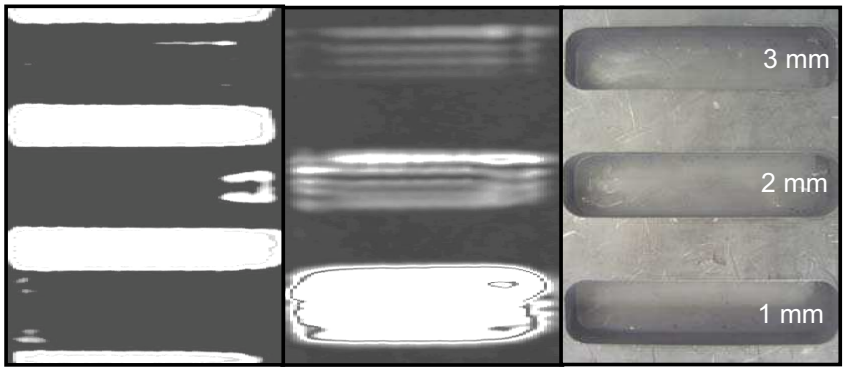

a) b) c)

Figure 3. Single-sided scans of hidden cavities in Al-sample (c) with AC-SAW (a) and AC-PAW (b).

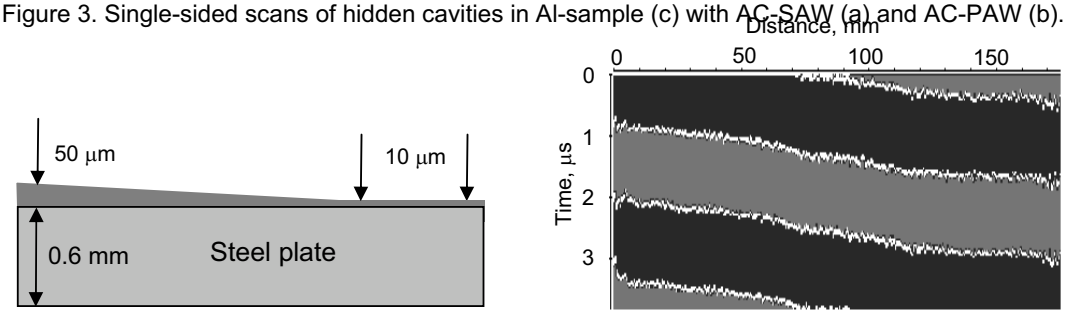

Figure 4. FST-profilometry: (left) configuration of paint coating; (right) FST-B-scan (white lines indicate positions of zero displacements).

Fig. 5 (left) shows the resulting $v_{PAW}(\alpha)$ polar plot obtained by $\theta_0(\alpha)$ measurements for a sample of uniaxial liquid crystal polymer. The "figure-of-eight" symmetry indicates a strong elastic anisotropy: the calculated plate wave velocities range from ≈520 m/s for α = 90° to ≈900 m/s for α = 0 -180° axis which reveals the direction of the highest stiffness. Another example of anisotropy measurements (Fig. 5, right) is concerned with a beech veneer wood laminate which comprises two unidirectional plies of equal thickness (≈ 600 μm) with their L-axis (fibre directions) rotated by 90^0. The cloverleaf velocity pattern confirms the expected 4-fold elastic symmetry in the cross-laminate.

2.2. Waveform imaging mode

An alternative approach to remote measurements of the velocity anisotropy is concerned with air-coupled wavefront imaging. It is based on the PAW and SAW excitation by a surface impact with a focused ACU-beam (*Figure 1, b*). For a point-like source (size of the excitation area smaller than a wavelength), the shape of the generated cylindrical wavefront is independent of the source geometry and is formed by the in-plane stiffness anisotropy of the material. A point-by-point scan of the sample surface using an optical interferometer enables to record and image the wavefront pattern and thus to monitor the material anisotropy. Besides, any defects in the observation area distort the wavefield and hence can also be detected this way [4].

In the wavefront imaging mode, a laser scanning vibrometer was used for detecting cylindrical air-coupled PAW and SAW. The output signal of the vibrometer was compared with the reference voltage to result in recording of the phase synchronized time traces of the vibration velocity for each position of the laser beam. The data acquired over the specimen surface are colour coded and played back as a time sequence of 2D-frames displaying an animated picture of wave propagation.

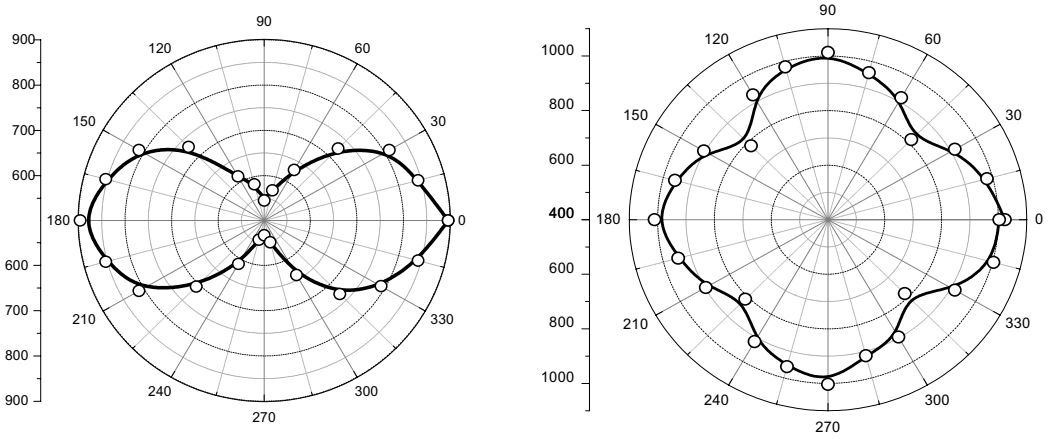

Figure 5. In-plane velocity anisotropy ($v_{PAW}(\alpha)$) measured in FST-mode: uniaxial liquid crystal polymer (left); [0-90^0] cross-ply of beech veneer (right).

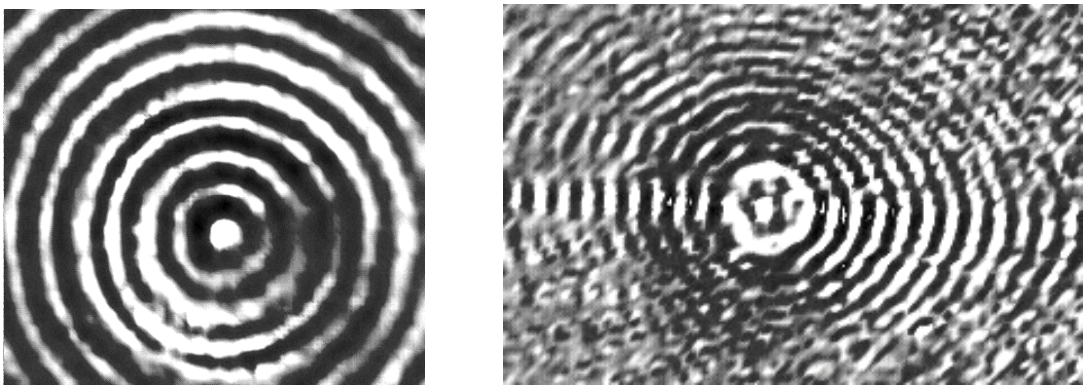

Figure 6. ACU wavefront imaging: SAW in 2-cm thick PMMA sample (left); PAW in a plate of uniaxial liquid crystal polymer (right).

Examples of wavefront imaging are given in *Fig*ure 6. As expected, for isotropic material (PMMA), the SAW wavefronts are close to ideal concentric circles (*Figure 6, left*). On the contrary, the in-plane stiffness anisotropy in a liquid crystal polymer distorts the wavefronts: one can see an evident elongation of the PAW wavefront along the fibre direction (horizontal axis in *Figure 6, right*). This image also demonstrates a high anisotropy of elastic wave dissipation due to a strong scattering in the direction normal to fibres. As a result, the wave energy is focused along the reinforcement direction ("phonon focusing"). Both effects make the wavefront imaging applicable for remote detection of local fibre directions in composite materials.

2.3. Nonlinear NDE with ACU conversion

Another new area of applications of the ACU is nonlinear NDE which is based on measurements of the wave propagation parameters beyond the limit of Hooke`s law. Local material nonlinearity strongly increases in damaged areas and, thus, is a very sensitive indicator of defect formation. A flexible operation of nonlinear NDE can be provided by using the ACU-conversion for non-contact acoustic wave excitation. In addition, the focused nonlinear ACU-option would benefit by probing nonlinearity locally and reading information directly out of the damaged areas.

For acoustic wave propagation in the medium with an ambient strain, the elastic nonlinearity results in a variation of wave velocity with static strain ε [3]:

$$c(\varepsilon) = c_0(1 - \beta_2\varepsilon - \frac{3}{2}\beta_3\varepsilon^2 - ...), \quad (1)$$

where c_0 is the wave velocity in an unstrained body, β_n are the parameters of nonlinearity whose values characterise the presence of defects in a material.

If in tensile tests, $c(\varepsilon)$ is measured locally in the expected fracture area, the damage induced can be revealed by measuring β_n as functions of static strain. Since a major contribution to $c(\varepsilon)$ is from the second-order terms, the parameter to be determined is: $\beta_2 = -(\partial c / \partial \varepsilon)/c_0$. Hence, one has to measure the local acoustic wave velocity as a function of static strain. The value of β_2 defines the rate of stiffness variation: positive values correspond to softening of the material while a negative sign means stiffening. Since the ACU-FST implements a local generation-detection of PAW, it can be applied for NDT of fracture by monitoring $\beta_2(\varepsilon)$ through a loading cycle.

In the experiment, $\beta_2(\varepsilon)$ was investigated for thermoplastic based composites fabricated by injection moulding [3]. The ACU-PAW velocity was derived from measurements of the FST-output phase variation. *Figure 7* shows the results of tensile tests for glass-fibre reinforced polypropylene

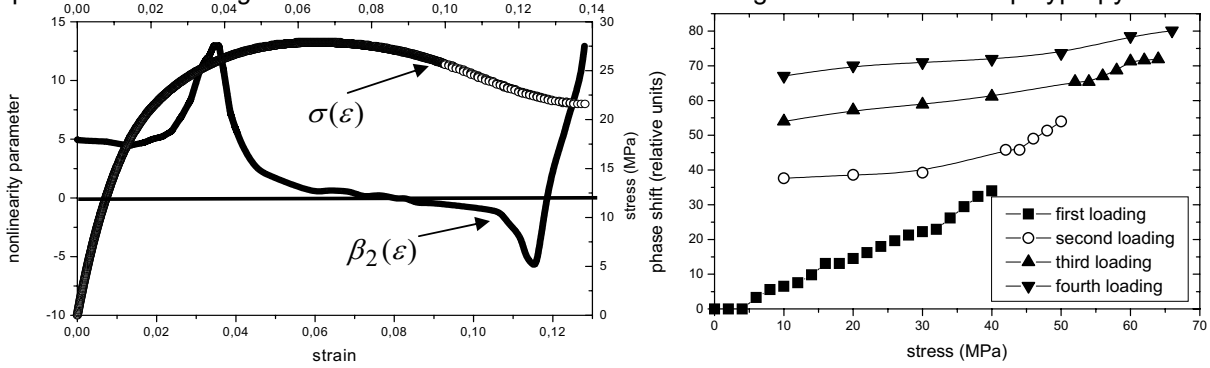

Figure 7. Stress-strain curves and $\beta_2(\varepsilon)$ for tensile loading of 5% GFRP (left); phase shift of FST-output for cyclic loading of glass fibre bundle embedded in a polycarbonate plate.

(5% weight fraction of short glass fibres) and the load applied normal to the fibre directions. In this case, the stress causes a high strain exclusively in the matrix regions between the transversal fibres. As a result, the deformation of the composite, basically, develops similarly to that of the polymer matrix: softening due to molecular untangling (positive β_2) is balanced by their straightening and alignment ($\beta_2 \to 0$). Stiffening of the matrix due to drawing and crazing makes β_2 negative that is a precursor of cracking and eventual quasi-ductile fracture. Further increase in ε, causes a substantial rise in positive β_2 which indicates material damage. Since the β_2 rise precedes the fracture, it can be used as a signal for oncoming failure.

In brittle materials and composites under cyclic loading, one would expect a hysteretic elastic behaviour of material because of crack accumulation with each consecutive cycle. To verify this assumption we measured the phase shift of the FST-output (proportional to PAW velocity) as a function of applied stress for a few loading cycles of glass fibre bundles embedded in a thin polycarbonate plate. Accumulation of irreversible damage is illustrated in *Figure 7, right,* where the measurements of $\Delta\varphi$ in the area of intensive cracking adjacent to the fibre ends are presented. A hysteretic elastic behaviour confirms irreversible damage induced by cyclic mechanical loading.

3. Conclusions

The ACU conversion into plate and surface waves provides new opportunities in remote linear and nonlinear NDE. The focused slanted modes demonstrate superior performance in imaging of defects, enable a high-accuracy profilometry of coatings and mapping of in-plane stiffness anisotropy. The wavefront imaging is applicable for a rapid interrogation of material anisotropy and, in particular, for remote monitoring of uniformity of fibre directions over large areas in composites. Fracture development in tensile and cyclic loading can be traced by using local nonlinear behaviour of air-coupled plate (or surface) wave propagation.

REFERENCES

[1] Rogovsky (A.). - *Development and application of ultrasonic dry-contact and air-contact C-scan systems for non-destructive evaluation of aerospace components.* Material Evaluation, **50**, 1991, p. 1491-1497.

[2] Luukkala (M.), Heikkili (P.), and Surakka (J.). - *Plate wave resonance – a contactless test method*. Ultrasonics, **9**, 1971, p. 201-208.

[3] Solodov (I.), Pfleiderer (K.), Gerhard (H.), Predak (S.), and Busse (G.). - *New opportunities for NDE with air-coupled ultrasound.* NDT&E, (in print, available online 22 August 2005).

[4] Solodov (I.), Pfleiderer (K.), and Busse (G.). - *Laser vibrometry of air-coupled Lamb waves: a novel methodology for non-contact material characterization.* Materialpruefung, **47**, 3, 2005, p. 3-7.